UDC 004.89 **doi:** https://doi.org/10.20998/3083-6298.2025.01.02

Fatih Bayir[1], Fuad Aliew[2]

[1] Gebze Technical University, Gebze, Kocaeli, Turkey
[2] Yeditepe University, Istanbul, Turkey

PERFORMANCE EVALUATION OF TYPE-2 FUZZY LOGIC CONTROLLER FOR A SENSORLESS VECTOR CONTROLLED BRUSHLESS MOTOR

Abstract. Topicality. Despite having some important features over other types of motors, due to their high non-linearity driving characteristics, controlling brushless motors may require some complex algorithms such as Vector Control (Field Oriented Control). In plants with high dynamic behavior and uncertainty, the control of these motors becomes even more sensitive. Under such conditions, vector control which consists conventional PID regulators may be insufficient. **The purpose of the article.** This study proposes a brushless motor drive with soft computing based vector control algorithm. **The following results were obtained**. A Type-2 Fuzzy Logic Controller (T2FLC) scheme for a sensorless vector-controlled brushless motor driver is presented. The study also aims to realize a comparison of performances between classical PI controllers and T2FLC, in the control of brushless motor systems where high dynamic characteristics and uncertainty situations are the two main problems. **Conclusion.** In the study, a Permanent Magnet Synchronous Motor (PMSM) is electrically modeled and a sensorless Field Oriented Control (FOC) scheme is applied to it. For closed loop speed control, both T2FLC and PI controllers are designed and their performance are compared to each other. All modeling and simulation study is realized in MATLAB/Simulink environment.

Keywords: field oriented control, vector control, soft computing, type-2 fuzzy logic control, artificial intelligence, PMSM speed control

1. Introduction

Over the last two decades, brushless motors have become more and more popular in many industrial field, due to their numerous advantages such as low torque ripple, durability, efficiency and small size [1].

Since these motors have no brush commutators, they need to be electronically commutated. Various driving techniques to control brushless motors have been studied over years. Brushless Direct Current motors (BLDC) and Permanent Magnet Synchronous motors (PMSM) are the main types of brushless motors. The control process of a BLDC motors is relatively straightforward, whereas more complex algorithms may be required to control PMSMs. The vector control is reputed as one of the most appropriate method to control PMSM motors efficiently [2, 3]. Vector Control algorithms can be realized in different forms such as Direct Torque Control (DTC) and Field Oriented Control (FOC) [4]. In this study, a sensorless FOC scheme for a PMSM is proposed.

In FOC algorithm, three phase stator currents are converted to two phase DC quantities by applying Clarke and Park Transformations, respectively. The main goal of the FOC technique is decoupling the stator currents into the torque generating and flux generating components by using these transformations [5]. Once these conversions are completed, the decoupled quantities are DC signals now, they can be easily regulated by a linear control technique such as PID controllers. However, PID controller or its derivatives (PI, PD etc.) lack the ability to cope with uncertainties. They also have low dynamic response and affected by non-linearity [6]. Furthermore, since the parameters are generally determined by trial and error or a specific method such as Ziegler - Nichols, these fixed parameters may not deliver satisfactory responses in highly dynamic systems. Besides, the Ziegler-Nichols method often causes large overshoot and oscillating responses. For all these reasons, PID controllers are not the wisest choice for controlling PMSM motors. It may be necessary to turn to intelligent control methods. As an intelligent control method, soft computing techniques are able to overcome non-linearity and promises computational simplicity. Genetic Algorithms (GA), Fuzzy Logic (FL) and Artificial Neural Networks (ANN) are the main soft computing techniques.

Fuzzy Logic enables us to solve issues caused by nonlinearity and uncertainty in a control application. It has a similar operation to human reasoning and presents a natural way to design functional blocks for an intelligent control system [7]. A complex system which cannot be easily transformed a mathematical model, can be expressed as a set of rules based on linguistic elements by using Fuzzy Logic. A decade after introduced the Fuzzy Logic controller, L. Zadeh announced the Type-2 FLC (T2FLC) in 1975. T2FLC shows better performance in managing uncertainties than T1FLCs. It also has better results in complex systems where robust or adaptive control is thought as only solution, to overcome uncertainty and parameter changes [8].

In FOC, rotor position angle is continuously needed to perform Park Transformation and Inverse Park transformation. This angle can be determined either by using a position sensor (Hall Effect sensors, incremental encoders or high resolution resolvers) or position estimators which uses no sensor [9]. In this study, a sensorless position detection technic is employed. Since classification or performance comparison of sensorless position detection techniques is outside of scope of this study, only the studied method will be discussed here: The Sliding Mode Observer based position estimator. It has some advantages over others, such as having simple structure and being free from motor parameters [10].

Studies combining sensorless FOC and T2FLC for a PMSM driver are scarce. Researchers have generally turned to the control of BLDC motors, which are relatively effortless. Ref [8] proposes Interval Type-2 Fuzzy Logic Controller for speed control of a DC Motor. Ref [11] presents comparative results of T1FLC and T2FLC speed controllers for BLDC motors. Ref [12] employs a Sensorless BLDC to control by T2FLC. It determines the rotor position with Zero Cross Detector. Ref [13-16], all deals with the performance of Type-1 FLC for PMSM with minor differences. Ref [17] gives detailed information about sensorless position estimation techniques for PMSM motors. Similarly, Ref [18] explains the various sensorless methods and realizes a performance comparison among them.

The paper is organized as follows. The next section presents a mathematical model for a PMSM in *dq* reference frame. In section 3, sensorless FOC is discussed. Section 4 deals with Sliding Mode Observer based position estimator. In Section 5, a Type-2 Fuzzy Logic Controller (T2FLC) is designed for closed loop speed control. Last two sections comprise simulation results and conclusion.

2. Mathematical model of PMSM

The rotor of a PMSM is made of permanent magnets that are mounted in such a way to produce sinusoidal back EMF in stator windings [19]. The electrical equivalent of a 3-phase PMSM can be represented as Figure 1.

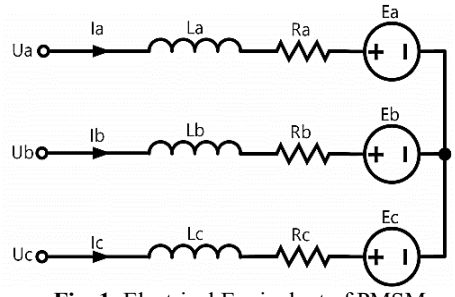

Fig. 1. Electrical Equivalent of PMSM

As seen in Figure 1, each stator phase of PMSM has own resistive, inductive and back-EMF components. In the modelling, it is pre-assumed that stator resistances are equal to each other (R_s=R_a=R_b=R_c) and mutual inductances are neglected. There are three types of PMSM modeling in different reference frame models. In this study, *dq* reference frame model is employed due to its simplicity. In Figure 2, *dq* electrical model of PMSM is shown. Note that in *dq* reference frame, the stator inductance is divided into two different inductances called L_d and L_q. In surface mounted PMSM (SPMSM), $L_d = L_q$ while in interior PMSM (IPMSM), $L_d < L_q$ [20]. In this study, an IPMSM is modeled which has non-equal L_d and L_q values.

According to Figure 2, the rotating *dq* frame based electrical equations can be written as follows

$$v_d = R_s.I_d + L_d.pI_d - L_q.\omega_e.I_q \quad (1)$$

$$v_q = R_s.I_q + L_q.pI_q + L_d.\omega_e.I_d + \omega_e.\Lambda_m \quad (2)$$

where ω_e – electrical speed, Λ_m – permanent magnet flux linkag, p – stands for derivative.

Note that in equations (1) and (2), the effects of magnetic saturation and magnetic hysteresis are neglected.

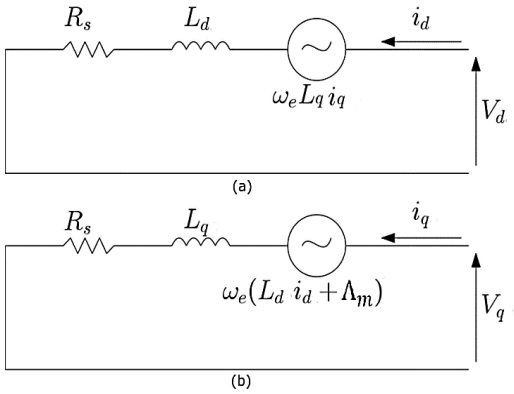

Fig. 2. PMSM electrical equivalent in d axis (a) and q axis (b) respectively

Mechanical Equations of PMSM in *dq* reference frame is defined by

$$T_e = \frac{3}{2}P\left(\Lambda_m I_q + \lambda_d I_q - \lambda_q I_d\right) \quad (3)$$

$$\omega_r = \frac{1}{J}\int (T_e - T_L - B\omega_r)dt \quad (4)$$

where T_e – electromechanical torque, P – pole number, J – inertia, B – friction coefficient, ω_r – mechanical rotor speed.

3. The FOC Scheme

In Figure 3, the block diagram of the proposed sensorless FOC scheme is shown. As depicted in Figure 3, the position angle of the rotor (Θ) is requisite to perform Park and Inverse Park Transformations. In sensorless position detection, the available position is determined not by sensors but by using some algorithms. In this study, a Sliding Mode Observer (SMO) model is performed to estimate the current position angle of the rotor. There are other sensorless position estimation methods yield varying performances in the market. However, SMO is chosen in this study due to its some advantages over other methods, as mentioned in the related section of the paper.

In FOC technique, there are two fundamental features that make it superior to other control methods, especially for driving AC fed machines. Firstly, FOC allows to decouple and regulate the current and flux magnitudes independently. The second one is, it can make possible to use linear closed loop control techniques, even at higher input frequencies [21]. Algorithm of the FOC can be summarized as follows:

- The 3-phase stator currents i_a, i_b and i_c are measured. i_c can be also calculated by using the Kirchhoff's Current Law ($i_a + i_b + i_c = 0$), without a third measurement.

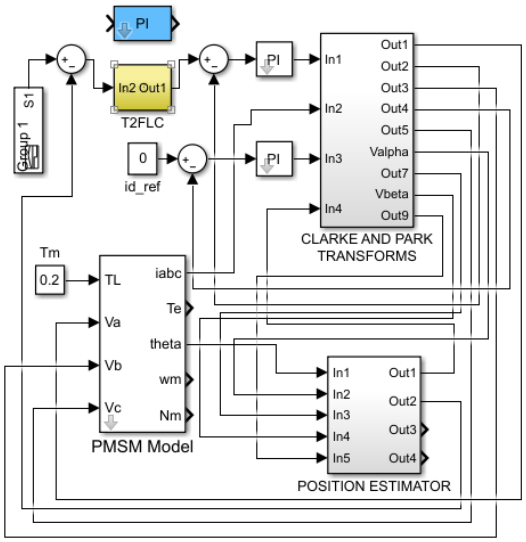

Fig. 3. General Block Diagram of the proposed sensorless FOC

- The Clarke Transformation is applied to the 3-phase currents (i_a, i_b and i_c). Two new orthogonal currents (i_α and i_β) in two-axis stationary coordinate system occur when the transformation ends. Thus, the transformation outputs the variables i_α and i_β using the measured quantities i_a, i_b and the calculated quantity i_c. Now, i_α and i_β are time-dependent quadrature current vectors from a stator perspective.
- The Park Transformation is applied to the orthogonal current vectors (i_α and i_β) and it provides two rotating current vectors (I_d and I_q) in a two-axis rotating coordinate system aligned with the rotor flux. I_d and I_q become constant while steady-state condition takes place. This means that these currents become DC quantities after the transformation is complete.
- Closed loop control is applied to I_d and I_q currents. The references of I_d and I_q currents regulate rotor magnetizing flux and torque output, respectively. The output of the controllers will yield the voltage vectors of V_d and V_q, as the input voltages for VSI after applying Inverse Park Transformation.
- The position estimator uses V_α, V_β, I_α and, I_β, to estimates a transformation angle. By this angle, the location of the next voltage vector is determined.
- By applying Inverse Park Transformation, each output of the current controllers of V_d and V_q are transformed back to the two-axis
- stationary coordinate using the estimated angle. V_α and V_β voltage vectors are determined after this transformation.
- The V_α and V_β voltages are converted to three-phase values of V_a, V_b, and V_c. These voltages are used to specify the next PWM duty cycle, achieving the required vector.

The equations of Clarke, Park and the Inverse Park transformations can be written as, respectively:

$$\begin{bmatrix} V_\alpha \\ V_\beta \end{bmatrix} = \begin{bmatrix} R.i_a + p.\lambda_a \\ \frac{1}{\sqrt{3}}\{R.(i_b - i_c) + p.\lambda_b - p\lambda_c\} \end{bmatrix} \quad (5)$$

$$\begin{bmatrix} v_d \\ v_q \end{bmatrix} = \begin{bmatrix} \cos\theta & \sin\theta \\ -\sin\theta & \cos\theta \end{bmatrix} . \begin{bmatrix} v_\alpha \\ v_\beta \end{bmatrix} \quad (6)$$

$$\begin{bmatrix} v_\alpha \\ v_\beta \end{bmatrix} = \begin{bmatrix} \cos\theta & -\sin\theta \\ \sin\theta & \cos\theta \end{bmatrix} . \begin{bmatrix} v_d \\ v_q \end{bmatrix} \quad (7)$$

4. SMO based Position Estimator

One of the most crucial criterions of the sensorless FOC algorithm is precise estimation of the rotor angle. As stated previously, rotor position angle is continuously needed to perform Park Transformation and Inverse Park Transformation. This angle can be determined by using position sensors such as Hall Effect sensors, incremental encoders or high resolution resolvers. However, using these sensors can increase the cost dramatically due to price of the sensors. Furthermore, mounting these sensors onto motor also enlarges the size of motor, rises labor and maintenance costs. Consequently, sensorless position detection techniques come into prominence.

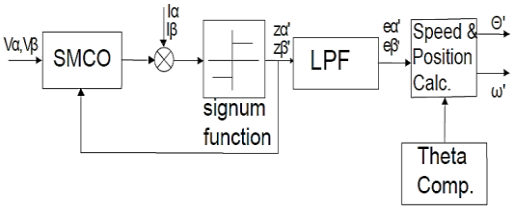

Fig. 4. Proposed Position Estimator based on Sliding Mode Observer

Many position detection techniques are available in the industry and all have varying advantages and disadvantages itself. Since classification or performance comparison of sensorless position detection techniques is outside of scope of this study, only the studied method will be discussed here. The Sliding Mode Observer (SMO) based position estimator is studied here because of its some advantages over others, such as having simple structure and being free from motor parameters. The proposed scheme of SMO based position estimator is shown in Figure 4.

As seen in Figure 4, SMO takes stator currents and voltages in αβ frame as inputs and calculates an estimated current of α and β axis. Then a bang-bang controller provides sliding gains, after the result is low pass filtered, estimated back EMFs can be obtained. Consequently, taking Inverse tangent of division of back EMF. The steps of algorithm of SMO position observer is as follows:

- Read the values $i_\alpha(n)$, $i_\beta(n)$, $v_\alpha(n)$, $v_\beta(n)$ in αβ axis.
- Calculate the estimated currents ($\hat{i}_{s\alpha}$, $\hat{i}_{s\beta}$) by using the following equation

$$\frac{d}{dt}.\hat{i}_s = A.\hat{i}_s + B(v^*_s - \hat{e}_s - z) \quad (8)$$

- Calculate the current errors by using following equation

$$\tilde{i}_s(n) = \hat{i}_s(n) - i_s(n) \quad (9)$$

- Obtain the z gain of the current observer by using the following equation

$$z = k.\,\text{sign}(\hat{i}_s - i_s) \quad (10)$$

- Estimate the BEMF ($\hat{e}_a$ and $\hat{e}_b$) by using by the following equation

$$\frac{d}{dt}.\hat{e}_s(n+1) = -\omega_0.\hat{e}_s(n) + \omega_0.z \quad (11)$$

- Obtain the estimated rotor position ($\hat{\Theta}_s$) by using the following equation

$$\hat{\Theta}_s = \tan^{-1}\left(-\frac{\hat{e}_{s\alpha}}{\hat{e}_{s\beta}}\right) \quad (12)$$

5. Type-2 Fuzzy Logic Controller

T2FLC is a modified version of T1FLC. Both controller structures are almost similar. The main difference between these controller is the defuzzification phase. Membership functions are classified as type-1 and type-2 since the clarification process is done with membership functions and they differ from each other structurally. One of the most important features that distinguishes T2FLC from T1FLC is type reduction [8].

Membership function of a Type-1 FLC can be defined as follows:

$$B = \left(x, \mu_B(x)\right) \mid \forall x \in X \quad (13)$$

where $\mu_B(x)$ – the membership level of variable x related to B set which is between 0 and 1.

This expression lacks the ability to define the uncertainty, since each variable x has a membership level between 0 and 1. Using Type-2 FLC becomes compulsory, if the membership level of a variable is not known or cannot be determined. Membership functions can be in different forms such as triangular, trapezoidal, Gaussian and sigmoid. In Figure 5, triangular membership functions for T1FLC and T2FLC are shown.

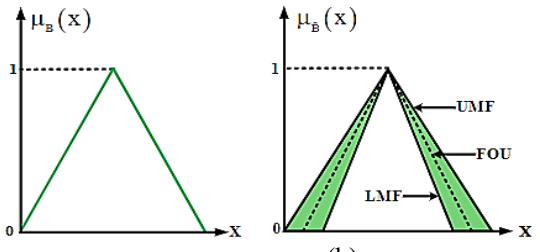

(a) (b)

Fig. 5. Triangular Membership functions a) T1FLC b) T2FLC

As seen in Figure 5, T2FLC has upper membership function (UMF) and lower membership function (LMF). The area between these two MFs is called the footprint of uncertainty (FOU). T2FLC is more robust than T1FLC since it can operate under a wider range of operating conditions than T1FLC. Also, T2FLC can cope with noise and load changes in a plant [11].

$\tilde{B}$ is the type-2 fuzzy set can be defined as following equations.

$$\tilde{B}\{(x, u, (\mu_{\tilde{B}}(x,u)) \mid \forall x \in x, \forall u \in J_x^u \subset [0,1]\} \quad (14)$$

$$\tilde{B} = \int_{x=X} \int_{u \in J_s} \mu_{\tilde{B}}(x,u)/(x,u) J_x \subseteq [0,1] \quad (15)$$

where X – the domain of the input variable, x – the value of the input variable, u – the primary grade of a type-2 fuzzy set, J_x – the primary membership of a type-2 fuzzy set, $\mu_{\tilde{B}}(x,u)$ – the secondary membership function [8].

$$\tilde{B} = \int_{x=X} \int_{u \in J_z} 1/(\mu_B(x,u) J_x \subseteq [0,1] \quad (16)$$

where $J_x \subseteq [0,1]$ and $\iint$ indicates the union over all acceptable x and u.

After defuzzification, the combination of all secondary sets can be defined as follows:

$$\tilde{B} = \int_{x \in X} \left[\int_{u \in J_x} f_x(u)/u\right]/x/ \quad J_x \subseteq [0,1] \quad (17)$$

After defuzzification in type-1, not a uniform geometric shape occurs for membership functions, while in type-2, a limited region with a uniform geometrical shape named FOU is occurred to express the membership functions in a better way. FOU can be described as follows.

$$FOU(\tilde{B}) = U_{x \in X} J_x \quad (18)$$

Figure 6 shows the general block diagram of T2FLC. One of main difference between T1FLC and T2FLC is the Type-Reducer block.

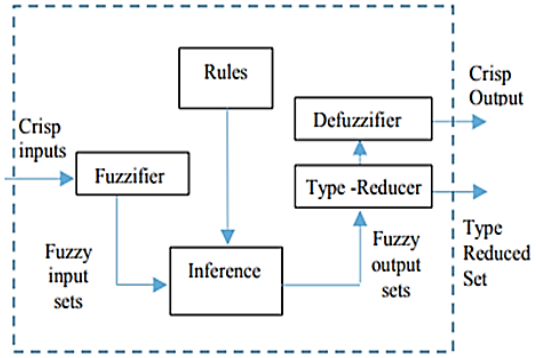

Fig. 6. T2FLC block diagram

Type reduction is the process of converting type-2 fuzzy sets to an equivalent type-1 fuzzy set. The Type-Reducer's accuracy is depended on the number of points taken into account in the input area of fuzzy sets. The more points are employed, the better results are obtained, however computational effort increases [12]. The proposed T2FLC has two inputs and one output. Inputs are the error and the change in the error, respectively. The error can be defined as the difference between the reference speed and the actual speed, which can be expressed as follows.

$$e(k) = [\omega_{ref}(k) - \omega(k)].G_{err} \quad (19)$$

The change in the error can be calculated by using derivative and it can be expressed as follows.

$$de(k) = [e(k) - e(k\text{-}1)].G_{derr} \quad (20)$$

where G_{err}, G_{derr} *and* G_u – the scaling factors.

The rule table is composed of 25 rules with 5 x 5 membership functions as shown in Figure 7.

e / de	NL	NS	Z	PS	PL
NL	NL	NL	NL	NS	Z
NS	NL	NS	NS	Z	PS
Z	NL	NS	Z	PS	PL
PS	NS	Z	PS	PS	PB
PL	Z	PS	PL	PL	PL

Fig. 7. Rule base of the proposed type-2 fuzzy logic controller

The FLC initially converts the crisp error and "change in error" variables into fuzzy variables and then are mapped into linguistic labels. Membership functions are associated with each label as shown in Figure 7 which consists of two inputs and one output. Inputs and output are triangular membership functions as shown in Figure 8 and Figure 9.

The error, "change in error" and output variables as labelled as NL, NS, Z, PS, PL which stands for negative large, negative small, zero, positive small and positive large, respectively. Membership functions for *e* and *de* inputs, and output are shown in Figure 8 and Figure 9 respectively.

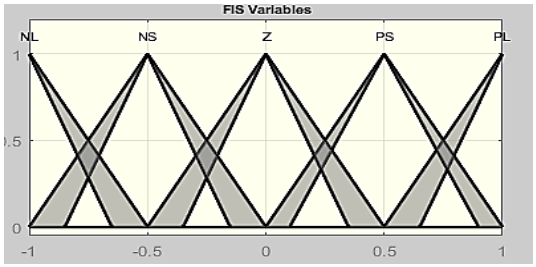

Fig. 8. Input Membership functions of error and change in error

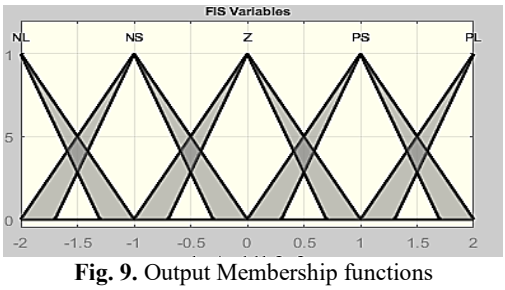

Fig. 9. Output Membership functions

Sugeno method is used as defuzzifier because of some advantages over Mamdani method such as being computationally efficient, working well with optimization, linear and adaptive techniques [22]. All calculations conducted by Matlab/Simulink T2FLC Toolbox which uses Takagi Sugeno -Kang (TSK) fuzzy inference system (FIS) [23].

6. Simulation Results

All modeling and simulations are conducted under MATLAB/Simulink environment. Modeled PMSM is assumed to have electrical parameters shown at table 1.

Table 1 – **Probability of task unloading**

Item	Quantity
Stator Resistance (R)	3.8Ω
Inductance (L_q)	2mH
Inductance (L_d)	2.5mH
Rotor Flux Constant (ψ)	0.1546V/rad/s
Moment of Inertia (J)	0.00176kgm2
Friction Vicious Gain (B)	0.0004Nm/rad/s
Number of Pole Pairs	4
Motor Power (W)	3kW

Simulations are carried out in three different case. Case 1,2 and 3 present the comparative results PI controller versus T2FLC for constant speed, variable speed and a step load applied the PMSM, respectively. Figure 10 shows the result for case 1 in where reference speed is set to a constant value of 1000RPM. It is aimed to see the performance of both controllers in terms of the transient response and steady state error.

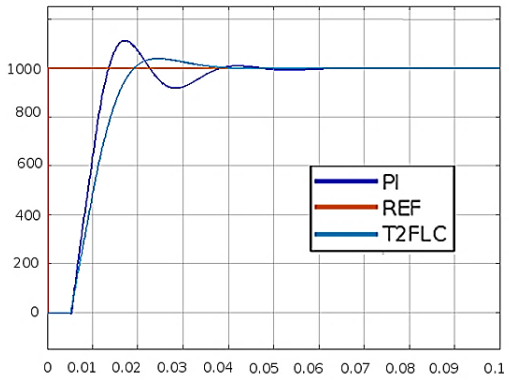

Fig. 10. Performance comparison of T2FLC over PI controller at the constant speed

As seen in Figure 10, T2FLC has less overshoot than PI controller (%3 and %10 respectively) and it reaches steady state more quickly. The settling time of T2FLC is 40ms while PI controller's is almost 60ms. Eventually, both controllers have no steady state error.

Figure 11 presents the result for case 2 in where the reference speed increases 400RPM to 1000RPM, then reduces to 600RPM. This case is intended to demonstrate the reference tracking performance of both controllers.

As Figure 11 shows, the reference speed is no longer constant. The motor rotates at an initial constant speed of 400RPM for 20ms, then continues at 1000RPM for the next 40ms, finally the speed drops to 600RPM. In this situation, both controllers track the reference speed without almost no steady state error. In terms of overshoot, the proposed T2FLC outperforms with a 2% overshoot, compared to PI controller which has a %7 overshoot. Similarly, while the reference speed drops,

T2FLC has way better performance than PI, in terms of overshoot and settling time.

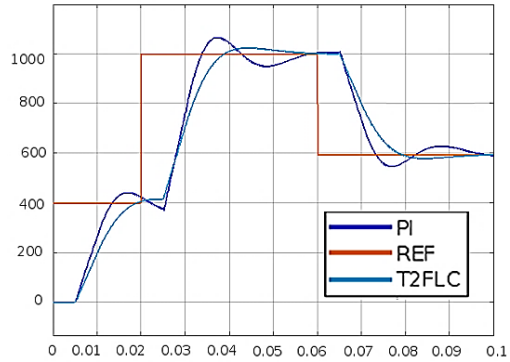

Fig. 11. Performance Comparison of T2FLC over PI controller at changing speed

In case 3, which is the last scenario, a load is applied to the PMSM in order to obtain disturbance rejection performance of the controllers. While PMSM rotates with a speed of 1000RPM, and as soon as it reaches steady state, a torque is applied at 55ms as shown in Figure 12.

As seen in Figure 12, the speed of the PMSM drops to 850 RPM in the PI controller, whereas it drops to 900 RPM in the T2FLC. In addition, T2FLC responds slightly faster than PI in following the reference speed. Thus, it can be concluded that the PI controller is more affected by disturbances than T2FLC.

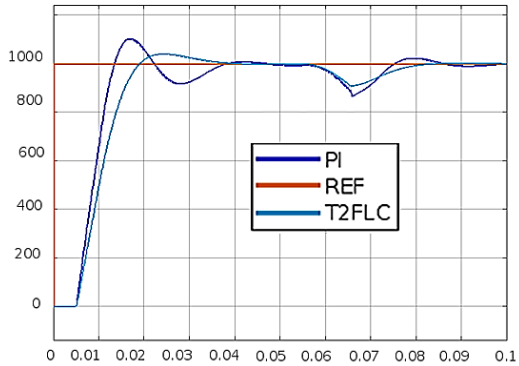

Fig. 12. Performance Comparison of T2FLC over PI controller when a load is applied to the motor

7. Conclusion

Position, speed and torque control of brushless motors, especially PMSMs, requires complex algorithms compared to other motor types. In this study, a comparison of traditional PI controller and Type-2F fuzzy logic controller, which is one of the soft computing control methods, is conducted for the speed performance of a sensorless vector controlled PMSM. According to the simulation results, the proposed T2FLC outperformed the PI controller in terms of the settling time, rise time, overshoot and steady state error. It is concluded from the simulation results that T2FLC shows a better dynamic performance and it can overcome the uncertainty. Also, PI controller is not capable to deliver satisfactory response in non-linear systems.

REFERENCES

1. Bose B. K. (1998), “Modern Power Electronics and AC Drives”, The University of Tennessee, Knoxville.
2. Krishnan R. (2002), “Electric Motor Drives Modeling, Analysis, and Control”, Prentice Hall of India Private Limited, New Delhi.
3. Sakunthala S., Kiranmayi R. and Mandadi P. N. (2018), “A Review on Speed Control of Permanent Magnet Synchronous Motor Drive Using Different Control Techniques”, *International Conference on Power, Energy, Control and Transmission Systems (ICPECTS),* Chennai, pp. 97-102, doi: 10.1109/ICPECTS.2018.8521574.
4. Gashtil H., Pickert V., Atkinson D., Giaouris D. and Dahidah M. (2019), “Comparative Evaluation of Field Oriented Control and Direct Torque Control Methodologies in Field Weakening Regions for Interior Permanent Magnet Machines”, *IEEE 13th International Conference on Compatibility, Power Electronics and Power Engineering (CPE-POWERENG)*, Sonderborg, Denmark, pp. 1-6, doi: 10.1109/CPE.2019.8862320.
5. Abuobeida E. Babikr, Mergani F.E. Rahman, Awadalla T. Ali, Abdelaziz Y. M. Abbas. (2015), “Indirect Field Oriented Control of Induction Motor Drive Using Fuzzy Controller”, *SUST Journal of Engineering and Computer Science (JECS)*, Vol. 16, No. 2.
6. Mitali Samal Das, Ranjan Soumya, and Bikash Pattnaik Chandra (2022), “Application of Soft Computing Techniques for Speed Control of Brushless DC Motors”, *International Journal of Electronics and Electrical Engineering,* Vol.4: Iss.1, Article2. DOI: 10.47893/IJEEE.2022.1180.
7. Rahul Malhotra, Singh Narinder, Singh Yaduvir (2011), “SOFT COMPUTING TECHNIQUES FOR PROCESS CONTROL APPLICATIONS”, *International Journal on Soft Computing (IJSC*), Vol.2, No.3, DOI: 10.5121/ijsc.2011.2303.
8. Acikgoz, H. (2018), “Speed Control of DC Motor Using Interval Type-2 Fuzzy Logic Controller”, *International Journal of Intelligent Systems and Applications in Engineering, IJISAE*, No 6(3), pp.197-202.
9. Mohamed A.S., Zaky M. S., Din A.S.Z., Yasin H.A. (2011), “Comparative Study of Sensorless Control Methods of PMSM Drives”, *Innovative Systems Design and Engineering,* Vol 2, No 5.
10. Saadaoui A., Khlaief M., Abassi A., Chaari and Boussak M. (2015), “Position sensorless vector control of PMSM drives based on SMO”, *16th International Conference on Sciences and Techniques of Automatic Control and Computer Engineering (STA*), Monastir, pp. 545-550, doi: 10.1109/STA.2015.7505148.
11. Abed H.Y., Humod A.T., Humaidi A.J. (2020), “Type 1 versus type 2 fuzzy logic speed controllers for brushless dc motors”, *International Journal of Electrical and Computer Engineering*, No 10(1), pp. 265-274, DOI:10.11591/ijece.v10i1.
12. Buyukyildiz C., Saritas I. (2020), “Sensorless Brushless DC Motor Control Using Type-2 Fuzzy Logic”, *Int J Intell Syst Appl Eng*, Vol. 8, No 4, pp. 184–190.
13. Mishra G., Dubey D., Joshi P., Agarwal and Sriavstava S. P. (2018), “A Complete Fuzzy Logic Based Real-Time Simulation of Vector Controlled PMSM Drive”, *2nd IEEE International Conference on Power Electronics, Intelligent Control and Energy*

Systems (ICPEICES), pp.809-814.
14. Lazi J. M., Ibrahim Z., Mat Isa S. N., Razali A. M., Rasin Z., and Kamisman N. (2016), "Fuzzy logic controller of PMSM for sensorless drives", *IEEE International Conference on Power and Energy (PECon*), pp. 540-545, doi: 10.1109/PECON.2016.7951620.
15. Qiping Chen, Sheng Kang, Liping Zeng, Qiang Xiao, Conghui Zhou, and Mingming Wu. (2020), "PMSM control for electric vehicle based on fuzzy PI", *International Journal of Electric and Hybrid Vehicles,* doi: 12. 75. 10.1504/IJEHV.2020.104251.
16. Maamoun Y. M., Alsayed and Shaltout A. (2013), "Fuzzy logic based speed controller for permanent-magnet synchronous motor drive", *IEEE International Conference on Mechatronics and Automation*, pp. 1518-1522, doi: 10.1109/ICMA.2013.6618139.
17. Benjak O, Gerling D. (2010), "Review of position estimation methods for IPMSM drives without a position sensor part I: Nonadaptive methods", *The XIX International Conference on Electrical Machines - ICEM 2010*, Rome, pp. 1-6, doi: 10.1109/ICELMACH.2010.5607978.
18. Tarmizi Y.A., Karim K.A., Tarusan S. A., Jidin A. (2017), "Review and Comparison of Sensorless Techniques to Estimate the Position and Speed of PMSM", *International Journal of Power Electronics and Drive System (IJPEDS*), Vol. 8, No. 3, pp. 1062-1069, DOI: 10.11591/ijpeds.v8i3. pp1062 1069.
19. Kongchoo Natthawut, Santiprapan Phonsit, Jindapetch Nattha (2020), "Mathematical Model of Permanent Magnet Synchronous Motor", *Asia Pacific Conference on Robot IoT System Development and Platform 2020 (APRIS2020)*, pp.69-70.
20. Murakami H., Honda Y., Kiriyama H., Morimoto S., and Takeda Y. (1999), "The performance comparison of SPMSM, IPMSM and SynRM in use as air-conditioning compressor", *Conference Record of the 1999 IEEE Industry Applications Conference*. *Thirty-Forth IAS Annual Meeting*, Phoenix, AZ, USA, Vol.2, pp. 840-845, doi: 10.1109/IAS.1999.801607.
21. Abassi M., Khlaief A., Saadaoui O., Chaari A., and Boussak M. (2015), "Performance analysis of FOC and DTC for PMSM drives using SVPWM technique", *16th International Conference on Sciences and Techniques of Automatic Control and Computer Engineering (STA)*, Monastir, pp. 228-233, doi: 10.1109/STA.2015.7505167.
22. Samed A.A.A., Fazli M.N., Salim N.A., Omar A.M.S., Osman M.K. (2017), "Speed Control Design of Permanent Magnet Synchronous Motor using Takagi-Sugeno Fuzzy Logic Control", *Journal of Electrical Systems*, Vol. 13, Issue 4, pp. 689-695.
23. Taskin A., Kumbasar T. (2015), "An open source Matlab/Simulink Toolbox for Interval Type-2 Fuzzy Logic Systems", *IEEE Symposium Series on Computational Intelligence – SSCI 2015*, Cape Town, South Africa. DOI: 10.1109/SSCI.20.

Received (Надійшла) 23.04.2025
Accepted for publication (Прийнята до друку) 14.05.2025

ВІДОМОСТІ ПРО АВТОРІВ/ ABOUT THE AUTHORS

Баір Фатіх – викладач, інженер, кандидат наук з електроніки, Гебзейський технічний університет, Гебзе, Туреччина;
Fatih Bayir – Teacher, Engineer, Ph.D candidate at Electronics, Gebze Technical University, Gebze, Turkey;
e-mail: f.aliew@yahoo.com; ORCID Author ID: https://orcid.org/0009-0003-0746-2179

Алієв Фуад – доктор технічних наук, професор, професор за програмою електронних технологій, Університет Єдітепе, Стамбул, Туреччина;
Fuad Aliew – Doctor of Technical Sciences, Professor, Professor Electronic Technology Program, Yeditepe University, Istanbul, Turkey;
e-mail: f.aliew@yahoo.com; ORCID Author ID: https://orcid.org/0000-0002-0153-7868;
Scopus ID: https://www.scopus.com/authid/detail.uri?authorId=44060941600

ОЦІНКА ПРОДУКТИВНОСТІ КОНТРОЛЕРА ТИПУ 2 З НЕЧІТКОЮ ЛОГІКОЮ ДЛЯ БЕЗДАТЧИКОВОГО ВЕКТОРНО-КЕРОВАНОГО БЕЗЩІТКОВОГО ДВИГУНА

Ф. Баір, Ф. Алієв

Анотація. Актуальність теми. Незважаючи на деякі важливі особливості порівняно з іншими типами двигунів, через їх високу нелінійність характеристик керування, керування безщітковими двигунами може вимагати деяких складних алгоритмів, таких як векторне керування (керування, орієнтоване на поле). В установках з високою динамічною поведінкою та невизначеністю керування цими двигунами стає ще більш чутливим. За таких умов векторне керування, що складається з традиційних ПІД-регуляторів, може бути недостатнім. **Мета статті.** У цьому дослідженні пропонується привід безщіткового двигуна з алгоритмом векторного керування на основі м'яких обчислень. Були отримані **наступні результати**. Представлена схема нечіткого логічного контролера (T2FLC) типу 2 для драйвера безщіткового двигуна з векторним керуванням без датчика. Дослідження також має на меті порівняти характеристики класичних ПІ-контролерів та T2FLC в керуванні системами безщіткових двигунів, де високі динамічні характеристики та ситуації невизначеності є двома основними проблемами. **Висновки.** У дослідженні електрично змодельовано синхронний двигун з постійними магнітами (PMSM) та застосовано до нього схему безчутливого керування, орієнтованого на поле (FOC). Для керування швидкістю в замкнутому контурі розроблено як T2FLC, так і ПІ-контролери, і їх характеристики порівнюються між собою. Усе моделювання та симуляційне дослідження реалізовано в середовищі MATLAB/Simulink.

Ключові слова: польово-орієнтоване керування, векторне керування, м'які обчислення, керування з нечіткою логікою 2-го типу, штучний інтелект, керування швидкістю з PMSM.